AJNR

Diffusion-Weighted MR Imaging Derived Apparent Diffusion Coefficient Is Predictive of Clinical Outcome in Primary Central Nervous System Lymphoma

R.F. Barajas, Jr, J.L. Rubenstein, J.S. Chang, J. Hwang and S. Cha

ORIGINAL RESEARCH

R.F. Barajas, Jr
J.L. Rubenstein
J.S. Chang
J. Hwang
S. Cha

🔓

Diffusion-Weighted MR Imaging Derived Apparent Diffusion Coefficient Is Predictive of Clinical Outcome in Primary Central Nervous System Lymphoma

BACKGROUND AND PURPOSE: There is evidence that increased tumor cellular density within diagnostic specimens of primary central nervous system lymphoma (PCNSL) may have significant prognostic implications. Because cellular density may influence measurements of apparent diffusion coefficient (ADC) by using diffusion-weighted MR imaging (DWI), we hypothesized that ADC measured from contrast-enhancing regions might correlate with clinical outcome in patients with PCNSL.

MATERIALS AND METHODS: PCNSL tumors from 18 immunocompetent patients, treated uniformly with methotrexate-based chemotherapy, were studied with pretherapeutic DWI. Enhancing lesions were diagnosed by pathologic analysis as high-grade B-cell lymphomas. Regions of interest were placed around all enhancing lesions allowing calculation of mean, 25th percentile ($ADC_{25\%}$), and minimum ADC values. Histopathologic tumor cellularity was quantitatively measured in all patients. High and low ADC groups were stratified by the median ADC value of the cohort. The Welch *t* test assessed differences between groups. The Pearson correlation examined relationships between ADC measurements and tumor cellular density. Single and multivariable survival analysis was performed.

RESULTS: We detected significant intra- and intertumor heterogeneity in ADC measurements. An inverse correlation between cellular density and ADC measurements was observed ($P < .05$). $ADC_{25\%}$ measurements less than the median value of 692 (low ADC group) were associated with significantly shorter progression-free and overall survival. Patients with improved clinical outcome were noted to exhibit a significant decrease in ADC measurements following high-dose methotrexate chemotherapy.

CONCLUSIONS: Our study provides evidence that ADC measurements within contrast-enhancing regions of PCNSL tumors may provide noninvasive insight into clinical outcome.

Primary central nervous system lymphoma (PCNSL) is a potentially curable brain tumor, the incidence of which is increasing among immunocompetent patients.[1-3] An overview of most clinical series suggests the existence of distinct prognostic subgroups of PCNSL with respect to response to high-dose methotrexate-based chemotherapy.[4] A significant fraction of patients with PCNSL often exhibit disease refractoriness to this treatment regimen.[4] The initial response to therapy, typically assessed at 4- to 6-week intervals after the initiation of methotrexate, is evaluated by measurement of tumor contrast-enhancement on MR imaging.[4-8] In general, 70% of PCNSL tumors exhibit radiographic evidence of tumor response; however, only

20%–40% of these patients experience prolonged progression-free survival (PFS) and overall survival (OS).

Given the significant long-term adverse effects associated with concurrent whole-brain irradiation, there is great interest in identifying prognostic subgroups of patients with PCNSL.[8] In particular, clinicians have sought to identify patients at low risk of recurrence who may simply be followed throughout the administration of chemotherapy without concurrent whole-brain irradiation. Conversely, patients at high risk for tumor recurrence may benefit from further chemotherapy or irradiation as a means of consolidation of response.[9,10]

At present, there are no established imaging biomarkers predictive of prognosis in patients with PCNSL. An imaging biomarker of tumor refractoriness to methotrexate-based chemotherapy would greatly facilitate clinical decisions and might lead to the early initiation of second-line salvage therapy in patients with high-risk PCNSL tumors, which could potentially lead to improved treatment strategies and clinical outcomes. Diffusion-weighted imaging (DWI) is an MR imaging technique that measures the diffusion rate of unbound extracellular water molecules.[11,12] Early investigations into DWI demonstrated that densely packed tumor cells with a high nuclear-to-cytoplasmic ratio could reduce water molecule motion.[11-14] It has been previously proposed that PCNSL can be histologically subclassified on the basis of cellular growth patterns into high and low cellular density tumors, which may have prognostic implications.[15,16]

Recently, it has been reported that DWI-derived apparent diffusion coefficient (ADC) measurements inversely correlate

with histopathologic assessment of PCNSL tumor cellular density.[14] To our knowledge, a relationship between pretherapeutic ADC measurements and clinical outcome in patients with PCNSL has not been previously reported. We, therefore, evaluated whether pretherapeutic ADC measurements could stratify patients with PCNSL into prognostic subgroups, allowing identification of patients whose tumors exhibited early disease progression and shortened overall survival.

Materials and Methods

Patient Population

Eighteen patients (10 men, 8 women; mean age, 57 ± 15 years; all immunocompetent) treated at the University of California San Francisco, between October 2001 and February 2009, were selected for this retrospective study on the basis of the following criteria: histopathologic diagnosis of PCNSL as defined by the World Health Organization; negative human immunodeficiency virus status; and absence of extra-central nervous system (CNS) lymphoma based upon CT scans of the chest, abdomen, and pelvis. All patients had a pathologic diagnosis of large B-cell CNS lymphoma and received identical methotrexate-based induction chemotherapy treatment. Notably, methotrexate is the only treatment-related variable that has been reproducibly positively associated with favorable outcome in PCNSL.[17] Of 70 patients who met the inclusion criteria for this investigation, only 18 were studied on the basis of having received pretherapeutic contrast-enhanced MR imaging of the brain with DWI. Twelve of the 18 patients had pretherapeutic, interval, and posttreatment follow-up contrast-enhanced MR imaging of the brain with DWI.

Each methotrexate treatment cycle was administered in the hospital setting. During induction, patients received methotrexate (3–8 g/m^2) every 14 days. In patients who achieved a complete response (CR), defined as resolution of contrast-enhancing lesions on follow-up MR imaging and, if indicated, by CSF cytologic analysis (if CSF cytology was positive for malignant cells at the time of diagnostic staging), to induction chemotherapy, 2–3 additional cycles of methotrexate (3–8 g/m^2) were administered every 14–21 days as consolidation therapy. Patients who achieved a partial response, defined as an interval decrease in contrast-enhancing lesion volume, or who exhibited disease progression, defined as an interval increase in contrast-enhancing lesion volume or the development of new enhancing lesions on follow-up contrast-enhanced MR imaging, were offered high-dose chemotherapy or whole-brain irradiation as salvage therapy. All patients with PCNSL included in this study underwent restaging with follow-up contrast-enhanced MR imaging within 5 cycles of methotrexate chemotherapy.[5]

MR Imaging Protocol

MR imaging data were obtained with a 1.5T clinical scanner (Signa Horizon, GE Healthcare, Milwaukee, Wisconsin). MR imaging examinations included conventional contrast-enhanced and DWI sequences obtained according to a standardized protocol: 3-plane localizer (TR/TE, 8.5/1.6 ms), sagittal T1-weighted spin-echo (TR/TE, 600/17 ms), axial 3D T2-weighted fast spin-echo (TR/TE, 3000/102 ms), axial fluid-attenuated inversion recovery (TR/TE/TI, 10,000/148/2200 ms), axial DWI echo-planar imaging (TR/TE, 10,000/99 ms; section thickness/intersection gap, 5/0 mm; matrix size, $256 \times 256 \times 24$; FOV, 24 cm; b-value, 1000 s/mm^2) acquired in the transverse plane throughout the infratentorial and supratentorial brain, and contrast-enhanced 3D spoiled gradient-recalled acquisition in the steady state

(SPGR) T1-weighted imaging (TR/TE, 34/8 ms; section thickness/intersection gap, 1.5/0 mm).

MR Image Processing

The contrast-enhanced 3D SPGR images and raw DWIs were transferred to a commercially available diffusion image-processing workstation (Advantage Workstation, GE Healthcare). Image processing was performed in a blinded manner by using commercially available software (FuncTool, GE Healthcare; R.F.B.). The contrast-enhanced 3D SPGR images were aligned to the same axial location and resolution as those of the DWIs. ADC maps were calculated on a voxel-by-voxel basis from the diffusion imaging sets. An example of the contrast-enhanced SPGR image, ADC map, and region-of-interest is shown in Fig 1. For each transaxial plane, a region of interest was manually defined around contrast-enhancing regions from the contrast-enhanced 3D SPGR image aligned to the DWI and ADC map, allowing ADC measurement and contrast-enhancing volume. The average of the mean (ADC$_{mean}$), 25th percentile (ADC$_{25\%}$), and minimum ADC (ADC$_{min}$) values for all regions of interest was calculated for all transaxial sections for each patient. In patients with multiple enhancing regions, regions of interest were placed around all enhancing regions, producing average ADC measurements derived from the entire enhancing tumor burden. The investigator responsible for the production of regions of interest was blinded to pathologic and clinical outcome (R.F.B.). All regions of interest were approved by an attending neuroradiologist certified by the American Board of Radiology with a Certificate of Added Qualification in neuroradiology (S.C.).

Histopathologic Analysis

All patients underwent surgical biopsy to establish the diagnosis of PCNSL. Diagnostic biopsy specimens were obtained from an enhancing tumor component. Hematoxylin-eosin−stained (HE) tumor specimens were qualitatively graded as low cellular density, defined as the presence of normal brain elements between tumor cells in the pathologic specimen; high cellular density, defined as the absence of normal brain elements between tumor cells in the pathologic specimen; or mixed cellular density, defined as a mixture of high and low cellular elements within the biopsy specimen (Fig 1).[15,16] Histopathologic analysis was performed independently by 2 separate investigators (R.F.B. and J.L.R.) blinded to biopsy location, MR imaging, and clinical outcome. Mean cellular density was quantitatively assessed for all biopsy specimens by manually counting and averaging the total number of HE-stained cell nuclei lying within a 5×5 ocular graticule grid covering an area of 0.25 mm^2 within 2−6 separate microscopic fields at a magnification of $\times 20$ (1.0 mm^2).[18]

Statistical Analysis

All ADC values are reported as 100×10^{-6} mm^2/s. High and low ADC groups were stratified by determining the median value from the cohort range of ADC$_{min}$ (384), ADC$_{25\%}$ (692), and ADC$_{mean}$ (854) measurements. Differences between groups were assessed by using a 2-sample Welch t test. This test generalizes the conventional t test by not prescribing that between-group variances are equal. A Pearson correlation was used to analyze the relationships between ADC values and biopsy specimen−derived cellular density.

The 3 clinical end points analyzed in this study were the following: radiographic response following treatment, PFS, and OS. Time to an event was calculated from the initiation of treatment until death (OS), progression or death (PFS), or date of last follow-up for patients without an event. Single covariate survival analysis was performed by us-
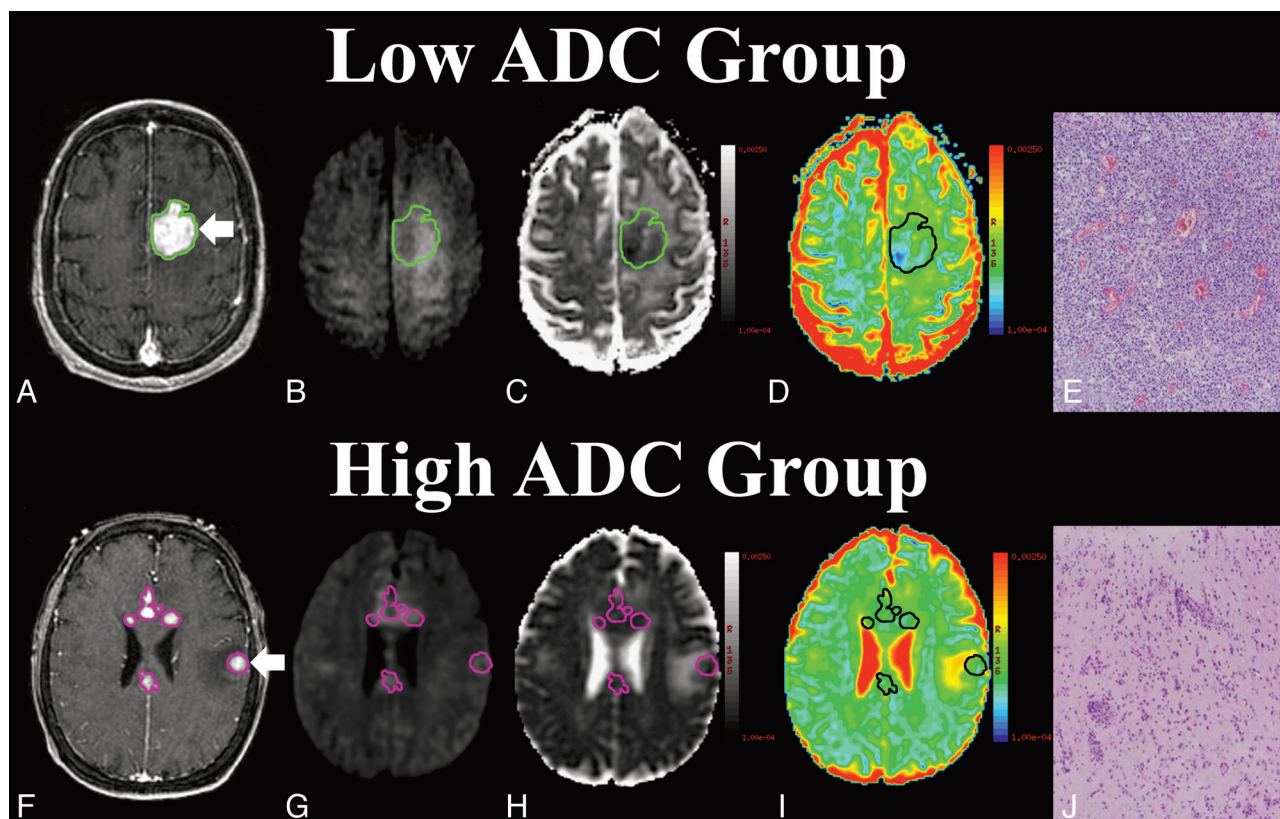
Fig 1. Comparison of diffusion-weighted imaging (DWI) and cellular density between high and low apparent diffusion coefficient (ADC) groups (*A* and *F*). Contrast-enhanced T1-weighted image with regions of interest surrounding enhancing regions that were pathologically diagnosed as primary central nervous system non-Hodgkin lymphoma. Arrow indicates enhancing region subjected to stereotactic biopsy. DWI (*B* and *G*), black and white ADC map (*C* and *H*), color ADC map (*D* and *I*), and biopsy specimens (*E* and *J*) from patient 2 (low ADC group) and patient 17 (high ADC group) (hematoxylin-eosin, original magnification ×100).

ing a logrank test. A Cox proportional hazard model was used for multivariable survival analysis. A Fisher exact test was used to investigate relationships between ADC group stratification and treatment response. A P value ≤ .05 was considered statistically significant.

Results

Tumoral ADC Heterogeneity and Patient Characteristics

Within the patient cohort, we identified a range in the distribution of intertumoral pretherapeutic ADC_{mean} (636–1016), $ADC_{25\%}$, (534–906), and ADC_{min} values (167–614) obtained from the entire enhancing burden of all PCNSL tumors. Given the evidence that ADC measurements may be influenced by the degree of intratumoral cellular density, we investigated whether a relationship exists between ADC measurements and clinical outcome in patients with PCNSL.[14-16] We focused on the ADC_{min} and $ADC_{25\%}$ on the basis of the assumption that these measurements best represent the most cellular component within contrast-enhancing tumor.

There was no statistically significant difference in major clinical prognostic factors, including age and performance status, when patients were stratified between high and low ADC groups ($P > .05$, Tables 1 and 2). Most important, the time between diagnosis and initial treatment, the time between treatment and follow-up MR imaging, the number of methotrexate treatment cycles between diagnosis and follow-up MR imaging, and the time between follow-up MR imaging examinations were not statistically different between high and low ADC groups ($P > .05$, Table 2).

Enhancing PCNSL Tumor Imaging Characteristics, ADC Measurements, and Correlation with Tumor Cellular Density

Pretherapeutic tumor enhancing volume was not statistically different between the low (mean, 11.0 ± 17.4 mL) and high (4.49 ± 2.61 mL) ADC groups ($P = .41$). Posttherapeutic tumor-enhancing volume was also found not to be statistically different between the low (8.45 ± 15.4 mL) and high (0.54 ± 0.63 mL) ADC groups ($P = .27$). Additionally, the change in enhancing volume observed between pre- and posttherapeutic imaging series was found not to be statistically significant (Table 2, $P = .37$).

A trend suggesting a relationship between ADC groups and treatment response was identified ($P < .01$, Fisher exact test). All 9 patients in the high $ADC_{25\%}$ group experienced a CR to methotrexate, while 7 of 9 patients in the low $ADC_{25\%}$ group experienced only a partial response or overt tumor progression within the first 2 months of follow-up. Of note, the 2 patients from the low $ADC_{25\%}$ group who did exhibit a CR to methotrexate-based therapy had higher $ADC_{25\%}$ values than other patients in the low group (Table 1).

Pretherapeutic ADC_{min}, $ADC_{25\%}$, and ADC_{mean} values within enhancing regions were significantly lower within the low ADC groups compared with the high ADC groups (Table 3). When comparing pre- and posttherapeutic ADC values, we noted that the differences in $ADC_{25\%}$ and ADC_{mean} values between these MR imaging examinations were statistically different between the low and high groups ($P < .04$, Table 3). Specifically,

Table 1: Clinical, imaging, and pathologic patient population characteristics[a]

Patient No.	ADC Group	Age (yr)/Sex	No. Enhancing Lesions	Response to Tx	ADC$_{25\%}$	ADC$_{min}$	ADC$_{mean}$	Overall Cellularity
1	Low	45/F	MP	PD	534	156	637	High
2	Low	82/F	SG	PD	541	167	745	High
3	Low	57/M	MP	PD	646	191	894	High
4	Low	61/M	MP	PR	528	214	877	High
5	Low	62/F	MP	PD	589	280	681	High
6	Low	54/M	MP	PD	638	338	749	Low
7	Low	70/M	SG	PR	623	367	719	High
8	Low	54/F	SG	CR	688	456	805	High
9	Low	26/M	SG	CR	692	398	835	High
10	High	52/F	MP	CR	693	294	779	Low
11	High	43/F	SG	CR	725	371	876	High
12	High	81/M	MP	CR	822	411	959	Low
13	High	53/F	MP	CR	831	414	873	Mixed
14	High	68/M	MP	CR	842	479	1016	Low
15	High	61/F	MP	CR	772	510	781	Low
16	High	53/M	MP	CR	741	525	891	Low
17	High	56/F	MP	CR	815	609	893	Mixed
18	High	67 mol/L	SG	CR	906	614	933	Low

Note:—ADC indicates apparent diffusion coefficient; MP, multiple; SG, single; Tx, treatment; PD, progressive disease; PR, partial response; CR, complete response; ADC$_{25\%}$, 25th percentile ADC value; ADC$_{min}$, minimum ADC value; ADC$_{mean}$, mean ADC value.
[a] Patients are stratified on the basis of the median 25th percentile value.

Table 2: Comparison of prognostic factors, cellular density, and clinical outcome[a]

	Age (yr)	MMSE	KPS	Days to Tx	Months to F/U MRI	No. Tx to F/U MRI	Change CE Volume	Months to Progression	Months to Death
Low ADC	56.7 (15.6)	25.2 (6.11)	62.2 (6.67)	13.8 (14.6)	8.3 (14)	2.00 (1.41)	2.50 (2.88)	9.4 (12.0)	15.8 (9.87)
High ADC	59.3 (11.3)	25.7 (4.50)	66.7 (5.00)	13.4 (11.7)	4.0 (8.0)	1.70 (0.70)	3.92 (2.39)	30.0 (18.0)	30.9 (17.0)
P value	.70	.83	.13	.94	.39	.53	0.37	<.01	.03

Note:—MMSE indicates pretherapeutic Mini-Mental State Examination score; KPS, Karnovsky performance status; Days to Tx, mean number of days between initial diagnosis by MR imaging and initiation of methotrexate-based chemotherapy; Months to F/U MRI, mean number of months between pre- and intratherapeutic MR imaging; No. Tx to F/U MRI, mean number of methotrexate treatments between pre- and intratherapeutic MR imaging; Change CE, difference in enhancing volume between pre-and posttherapeutic imaging series; Months to Progression, mean number of months to progression based on MR imaging if event occurred; Months to Death, mean number of months to death if event occurred.
[a] All data are presented as mean (± SD). Patients are stratified based on median 25th percentile value.

Table 3: Comparison of MR imaging findings[a]

	ADC$_{min}$	Change ADC$_{min}$	ADC$_{25\%}$	Change ADC$_{25\%}$	ADC$_{mean}$	Change ADC$_{mean}$
Low ADC	258 (109)	−18.7 (219)	608 (62)	84.7 (114)	771 (87.7)	116 (106)
High ADC	469 (107)	−120 (224)	794 (67)	−55.5 (84.7)	889 (77.0)	−42 (74)
P value	<.01	.31	<.01	.04	<.01	.01

Note:—Change ADC$_{min}$ indicates the difference between pre- and posttherapeutic ADC$_{min}$ values (negative values signify net decrease in value); Change ADC$_{25\%}$, difference between pre- and posttherapeutic ADC$_{25\%}$ values; Change ADC$_{mean}$, difference between pre- and posttherapeutic ADC$_{mean}$ values.
[a] All data are presented as mean (SD). All ADC values are reported as 100×10^{-6} mm^2/s.

the high ADC$_{25\%}$ and ADC$_{mean}$ groups tended to exhibit a net decrease in ADC values between pre- and posttherapeutic follow-up MR imaging, while the low ADC$_{25\%}$ and ADC$_{mean}$ groups exhibited a net increase in ADC values (Table 3).

Quantitative analysis of cellular density was performed in a blinded manner independently by 2 investigators on diagnostic PCNSL tissue specimens obtained from enhancing tumor components for all 18 patients. An inverse correlation between cellular density and ADC$_{25\%}$ ($R = -0.47, P = .05$) and ADC$_{mean}$ ($R = -0.54, P = .02$) values was identified (Fig 2).

### Pretherapeutic ADC Measurements Are Predictive of Clinical Outcome

Seven of the 18 patients exhibited either partial response or primary refractory disease with overt tumor progression within 4 methotrexate treatments administered in 2-week intervals. The ADC values for these 7 patients with primary refractory disease were significantly lower than those for patients whose tumors exhibited a CR: ADC$_{mean}$ ± SD (757 ± 96

versus $876 \pm 74, P = .02$), ADC$_{25\%}$ (586 ± 51 versus $774 \pm 74, P < .01$), and ADC$_{min}$ (244 ± 84 versus $462 \pm 98, P < .01$). Two of the 11 patients with an initial CR ultimately progressed, at 8 and 18 months, respectively (Fig 3A). Overall, 7 patients died as a result of progressive disease (Fig 3B). The mean follow-up time for all 18 patients in this study was 23.3 months (range, 1.1–57.3 months). The mean follow-up time for surviving patients was 27.5 months (range, 3.5–57.3 months).

Patients with enhancing tumors that contained ADC$_{25\%}$ values of <692 (low ADC group) experienced earlier disease progression and shorter overall survival despite identical chemotherapeutic treatment compared with that received by patients in the high ADC group. Patients in the low ADC group had greatly increased risk for both progression ($P = .03$, hazard ratio = 0.21) and death ($P = .02$, hazard ratio = 0.12) compared with the high ADC group (Table 2). Mean progression-free survival was also significantly shorter in the low ADC group compared with the high ADC group (Table 2). When we stratified patient outcome by median ADC$_{min}$ values (384), the PFS ($P = .01$, hazard ratio =
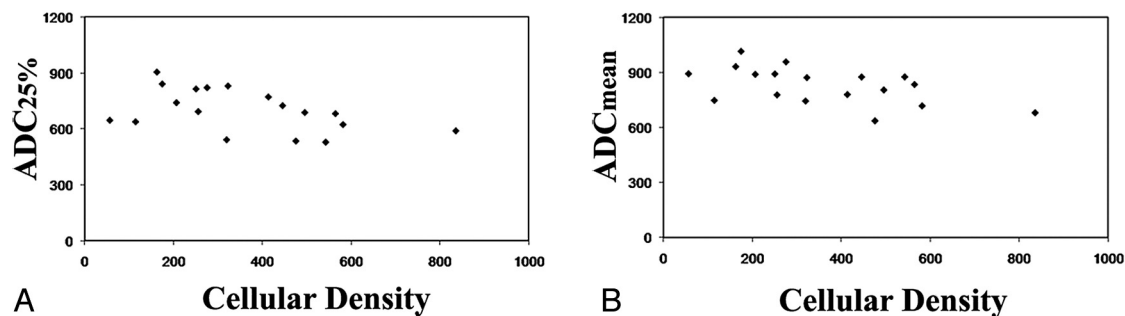
Fig 2. Scatterplots of cellular density measurements versus 25th percentile (ADC$_{25\%}$, A) and mean ADC (ADC$_{mean}$, B) values within contrast-enhancing tumor regions for all 18 subjects included in this study, demonstrating statistically significant inverse correlations (ADC$_{25\%}$, $R = -0.47$, $P = .05$; ADC$_{mean}$, $R = -0.54$, $P = .02$).
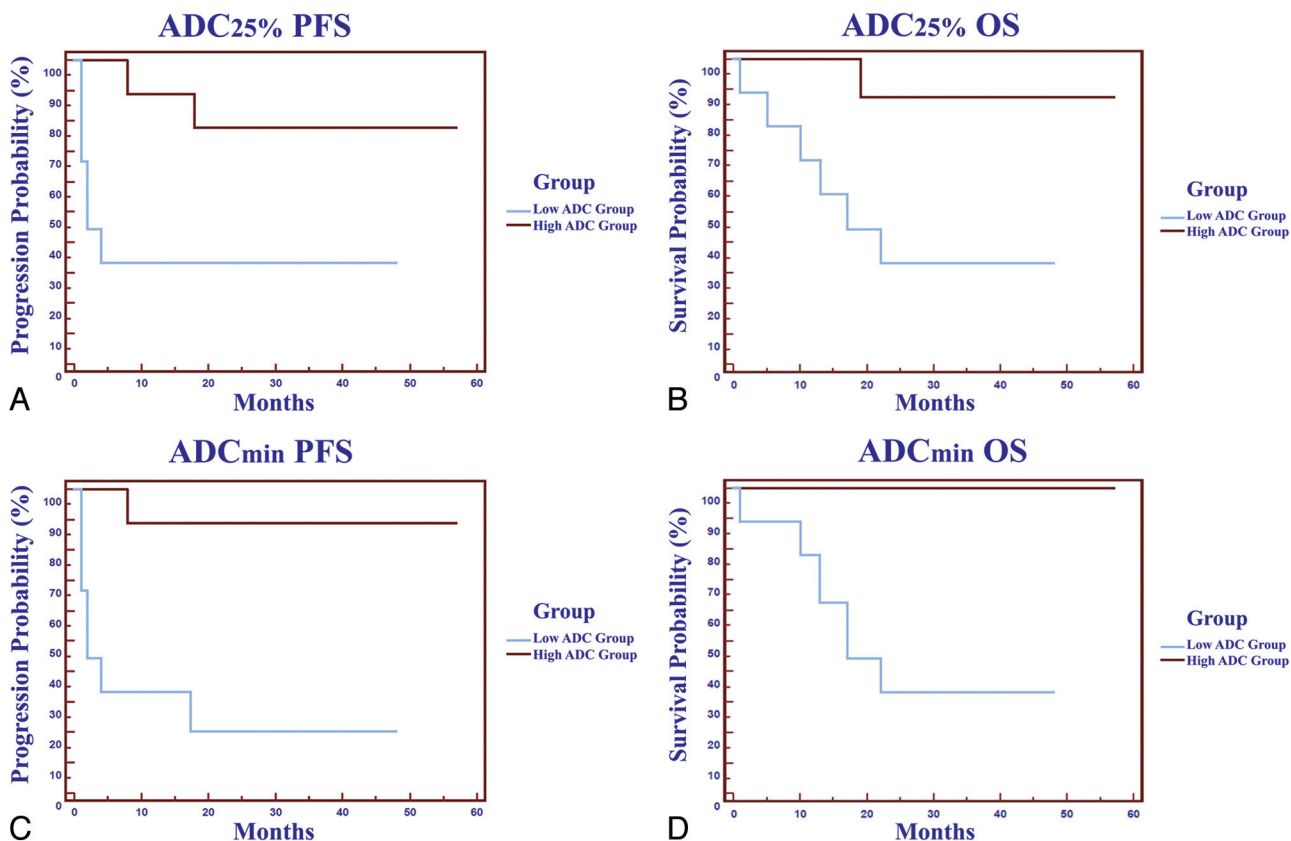
Fig 3. A and B, Patient outcome as a function of ADC$_{25\%}$ stratification into low and high groups. Kaplan Meier analysis (A) of progression-free survival (PFS) for patients stratified into the low ADC$_{25\%}$ group (<692, blue line) with a mean progression time of 9.4 months versus those stratified into high ADC$_{25\%}$ group (>692, red line) with a mean progression time of 30.0 months ($P = .02$, logrank test). Kaplan Meier plot (B) of overall survival (OS) for patients stratified into the low ADC$_{25\%}$ group (<692, blue line) with a mean survival of 15.8 months versus those stratified into high ADC$_{25\%}$ group (>692, red line) with a mean survival of 30.9 months ($P = .01$, logrank test). C and D, Patient outcome as a function of minimum ADC value shows a statistically significant difference in PFS and OS between low and high groups ($P < .05$).

0.08) and OS ($P = .01$, hazard ratio = 0.01) were significantly different between high and low ADC groups.

Patient outcome was observed to cluster into nonbimodal cohorts on the basis of ADC cutoff values (minimum, 375; 25th percentile, 700). When stratifying patient outcome by an ADC$_{min}$ value of 375, the PFS and OS were significantly different between high and low ADC groups ($P < .01$). Patient stratification based on an ADC$_{25\%}$ cutoff value of 700 revealed a significant difference in PFS ($P = .02$) and OS ($P < .01$) between high and low ADC groups.

Single covariate analysis of tumor cellular density and clinical prognostic factors in PCNSL, such as age (<60 versus ≥60 years), total volume of enhancing lesion (<10 mL

versus ≥10 mL), number of enhancing lesions (single versus multiple), lesion location (infra- versus supratentorial involvement), presenting Mini-Mental State Examination (MMSE) score (<25 versus ≥25), and Karnovsky performance status (KPS) (<70 versus ≥70) did not influence PFS or OS ($P > .05$). Multivariate analysis incorporating tumor cellular density and common prognostic factors (age, total volume of enhancing lesion, number of enhancing lesions, lesion location, presenting MMSE score, and KPS) and ADC$_{min}$ (<384 versus >384) or ADC$_{25\%}$ (<692 versus >692) suggested that pretherapeutic ADC value and KPS were the only factors predictive of clinical outcome ($P < .05$).

Discussion

In this study, we found that pretherapeutic ADC tumor measurements within contrast-enhancing regions were predictive of clinical outcome in patients with PCNSL. Specifically, we found that $ADC_{25\%}$ (<692) and ADC_{min} (<384) values were predictive of shorter PFS and OS. Additionally, an inverse correlation was found between ADC measurements and tumor cellular density. Finally, we found that patients with prolonged PFS and OS had a significant reduction in post-therapeutic ADC values.

Currently, there are no established imaging biomarkers predictive of clinical outcome in patients with PCNSL, a potentially curable disease. In our study, stratification of patients with PCNSL by pretherapeutic ADC measurements retrospectively provided a robust measure of eventual clinical response to treatment and overall survival. This correlation was preserved even when other known prognostic variables were taken into account. To our knowledge, the use of pretherapeutic ADC values as a predictive factor of the clinical outcome in PCNSL has not been previously reported. The ability to identify patients at risk for primary refractory disease by using pretherapeutic ADC measurements has important clinical implications. A noninvasive pretherapeutic imaging biomarker able to accurately identify patients at high risk for tumor refractoriness to methotrexate-based chemotherapy could greatly facilitate clinical decision-making, allowing the initiation of individualized second-line salvage therapies, which may result in improved clinical outcome.[9,10,19,20]

Poor clinical outcome in patients with PCNSL treated with high-dose methotrexate chemotherapy has been positively correlated with increased intratumoral expression of activated STAT6 within high-density tumors based on histopathologic analysis of diagnostic tissue specimens.[15,16,21] Quantification of STAT6 expression levels may eventually prove to be a sensitive and specific biomarker of clinical outcome; however, its analysis requires an invasive procedure and is not currently widely clinically available. The results of our study indicate that DWI-derived ADC measurements could potentially be used as a noninvasive imaging biomarker for identifying PCNSL tumors of high cellular density, which are at high risk for refractoriness to conventional high-dose methotrexate-based induction strategies.

In this study, we detected an inverse correlation between ADC measurements and tumor cellular density. Specifically, lower ADC values were correlated with increasing tumor cellular density. The results from our study are essentially in agreement with those of previous investigations. ADC values have been noted to be markedly reduced in PCNSL compared with other enhancing intra-axial tumors.[11-14,22-26] Guo et al[14] reported that ADC values were inversely related to tumor nuclear-to-cytoplasmatic ratios in their study of water diffusivity within PCNSL and high-grade astrocytomas.

Increased tumor cell density (as determined by counting lymphoma cell nuclei/high-power field from diagnostic brain biopsies) was found not to be a statistically significant predictor of clinical outcome. Additionally, a multivariable analysis of ADC measurements and tumor cell density found ADC to be the only predictor of clinical outcome. An important limitation of the quantification of tumor cell density by using microscopy in lymphoma is the inherent variability in the size and morphology of diffuse proliferations of large lymphoid cells. For this reason, we have also qualitatively defined tumor cell density on the basis of whether normal brain elements (neurons and glia) are detectable between the neoplastic cells within the pathologic specimen.[16] Our results suggest that while ADC measurements correlate with tumor cell density, DWI is a more accurate predictor of clinical outcome, given the capacity of this technique to summate additional unidentified prognostic biologic features of tumor aggressiveness beyond cell density.

ADC measurements often facilitate the clinical differentiation of PCNSL from high-grade glioma and intra-axial metastatic disease.[11-14,22-26] The ability to presumptively diagnose PCNSL on the basis of noninvasive molecular biomarkers as well as MR imaging may have a significant impact on clinical management. Unlike high-grade glioma, gross total surgical resection of enhancing regions offers no significant improvement in clinical outcome in patients with PCNSL.[27-30] The need to establish a definitive diagnosis necessitates tissue acquisition via stereotactic biopsy. Often clinicians rely on conventional anatomic contrast-enhanced MR imaging without using physiologic MR images, such as ADC measurements, when targeting enhancing tumor for biopsy. The results of our study suggest that localization of tumor regions with the lowest ADC measurements may allow the collection of pathologic specimens of highest potential prognostic significance and may minimize the rate of false-negative biopsy collection. Our results indicate that tissue sampling by using ADC-guided stereotactic biopsy in patients suspected of having PCNSL is an application worthy of further investigation.

In this study, we found that patients stratified to the high ADC group who subsequently were found to have improved PFS and OS were noted to exhibit a significant decrease in ADC measurements following high-dose methotrexate chemotherapy. This decrease in ADC measurements could be suggestive of a net reduction of extracellular water molecular motion within treated lesions. We hypothesize that this decrease may, in part, be due to greater tumor cellular responsiveness to methotrexate-based chemotherapies within the high ADC group. This improved response may subsequently lead to treatment-induced cellular swelling, resulting from diminished cellular water homeostasis, which may lead to a decrease in extracellular space within contrast-enhancing regions.[31]

Several other studies have demonstrated change in post-therapeutic ADC values following radiation and chemotherapy in primary glial brain tumors.[31-34] In a study of patients with unresectable glioma, Moffat et al[31] used ADC-derived functional diffusion maps (fDMs) to monitor contrast-enhancing regions during the course of therapy. The fDMs were found to predict patient response at 3 weeks from the start of treatment, revealing that early changes in tumor diffusion values could be used as a prognostic indicator of subsequent volumetric tumor response.[34] While fDMs have been suggested to be an early biomarker of eventual radiographic response in primary glial brain tumors, their utility as biomarkers in PCNSL has not previously been reported.

The use of serial ADC measurements in patients with PCNSL may have significant clinical implications. Currently, the response to methotrexate-based therapy is monitored by serial contrast-enhanced anatomic MR imaging. Increased enhancing volume has been correlated with worsened patient outcomes; however, clinical signs of disease refractoriness

can occur before the manifestation of progressive contrast enhancement on serial follow-up MR imaging.[4-7] The results of our study suggest that the use of serial ADC measurements in conjunction with contrast-enhanced anatomic MR imaging may be clinically useful in assessing early response to methotrexate-based treatment in patients with PCNSL.

Our study had several limitations. First, the results of our study may have been influenced by its relatively small sample size and retrospective nature. Second, because post-therapeutic biopsy samples are not normally obtained, we were unable to determine the pathophysiologic basis for the observed changes in ADC values on posttherapeutic MR imaging. We suggest that future studies may use image-guided stereotactic biopsy techniques to directly correlate tissue specimen characteristics with ADC measurements.

The technique for measuring ADC values described in this study was chosen to investigate PCNSL because it is robust and timely and clinically feasible. The image processing software and MR scanners used in this study are commercially available and frequently used in the clinical interpretation of MR images because DWI has become a standard imaging sequence in the evaluation of many diseases.

Conclusions

Currently, there are no established imaging biomarkers that are prognostic of clinical outcome in patients with PCNSL. The results of our study suggest that pretherapeutic tumor ADC measurements may noninvasively predict clinical outcome in patients with PCNSL. We suggest that future studies apply image-guided stereotactic biopsy techniques to directly correlate tissue specimen characteristics with ADC measurements. Additional studies are needed to prospectively validate these preliminary observations to determine the impact of ADC measurements in facilitating pathologic diagnosis, prognostication, and treatment planning.

References

1. *Statistical Report: Primary Brain Tumors in the United States, 1998–2002.* Hinsdale, Ilonois: Central Brain Tumor Registry of the United States; 2005
2. Surawicz TS, McCarthy BJ, Kupelian V, et al. **Descriptive epidemiology of primary brain and CNS tumors: results from the Central Brain Tumor Registry of the United States, 1990–1994.** *Neuro Oncol* 1999;1:14–25
3. Olson JE, Janney CA, Rao RD, et al. **The continuing increase in the incidence of primary central nervous system non-Hodgkin lymphoma: a surveillance, epidemiology, and end results analysis.** *Cancer* 2002;95:1504–10
4. Hochberg F, Baehring J, Hochberg E. **Primary CNS lymphoma.** *Nat Clin Pract Neurol* 2007;3:24–35
5. Abrey LE, Batchelor TT, Ferreri AJ, et al, for the International Primary CNS Lymphoma Collaborative Group. **Report of an international workshop to standardize baseline evaluation and response criteria for primary CNS lymphoma.** *J Clin Oncol* 2005;23:5034–43. Epub 2005 Jun 13
6. Glass J, Gruber ML, Cher L, et al. **Preirradiation methotrexate chemotherapy of primary central nervous system lymphoma: long-term outcome.** *J Neurosurg* 1994;81:188–95
7. Gavrilovic IT, Hormigo A, Yahalom J, et al. **Long-term follow-up of high-dose methotrexate-based therapy with and without whole brain irradiation for newly diagnosed primary CNS lymphoma.** *J Clin Oncol* 2006;28:4570–74
8. Abrey LE, DeAngelis LM, Yahalom J. **Long-term survival in primary CNS lymphoma.** *J Clin Oncol* 1998;16:859–63
9. Rubenstein JL, Fridlyand J, Abrey L, et al. **Phase I study of intraventricular administration of rituximab in patients with recurrent CNS and intraocular lymphoma.** *J Clin Oncol* 2007;25:1350–56. Epub 2007 Feb 20
10. Soussain C, Hoang-Xuan K, Taillandier L, et al. **Intensive chemotherapy followed by hematopoietic stem-cell rescue for refractory and recurrent primary CNS and intraocular lymphoma.** *J Clin Oncol* 2008;26:2512–18
11. Le Bihan D, Turner R, Douek P, et al. **Diffusion MR imaging: clinical applications.** *AJR Am J Roentgenol* 1992;159:591–99
12. Rowley HA, Grant PE, Roberts TP. **Diffusion MR imaging: theory and applications.** *Neuroimaging Clin N Am* 1999;9:343–61
13. Le Bihan D, Breton E, Lallemand D, et al. **MR imaging of intravoxel incoherent motions: application to diffusion and perfusion in neurologic disorders.** *Radiology* 1986;161:401–07
14. Guo AC, Cummings TJ, Dash RC, et al. **Lymphomas and high-grade astrocytomas: comparison of water diffusibility and histologic characteristics.** *Radiology* 2002;224:177–83
15. Rubenstein J, Shen A, Batchelor T, et al. **Differential gene expression in central nervous system lymphoma.** *Blood* 2009;113:266–67
16. Rubenstein, J, Fridlyand, J, Shen, A., et al. **Gene expression and angiotropism in primary CNS lymphoma.** *Blood* 2006;107:3716–23
17. Blay JY, Conroy T, Chevreau C, et al. **High-dose methotrexate for the treatment of primary cerebral lymphomas: analysis of survival and late neurologic toxicity in a retrospective series.** *J Clin Oncol* 1998;16:864–71
18. Burger PC, Shibata T, Kleihues P. **The use of the monoclonal antibody Ki-67 in the identification of proliferating cells: application to surgical neuropathology.** *Am J Surg Pathol* 1986;10:611–17
19. Matsumoto Y, Horiike S, Fujimoto Y, et al. **Effectiveness and limitation of gamma knife radiosurgery for relapsed central nervous system lymphoma: a retrospective analysis in one institution.** *Int J Hematol* 2007;85:333–37
20. Ryken TC, Meeks SL, Pennington EC, et al. **Initial clinical experience with frameless stereotactic radiosurgery: analysis of accuracy and feasibility.** *Int J Radiat Oncol Biol Phys* 2001;51:1152–58
21. Roy S, Josephson SA, Fridlyand J, et al. **Protein biomarker identification in the CSF of patients with CNS lymphoma.** *J Clin Oncol* 2008;26:96–105
22. Ducreux D, Wu RH, Mikulis DJ, et al. **Diffusion-weighted imaging and single-voxel MR spectroscopy in a case of malignant cerebral lymphoma.** *Neuroradiology* 2003;45:865–68
23. Stadnik TW, Chaskis C, Michotte A, et al. **Diffusion-weighted MR imaging of intracerebral masses: comparison with conventional MR imaging and histologic findings.** *AJNR Am J Neuroradiol* 2001;22:969–76
24. Kitis O, Altay H, Calli C, et al. **Minimum apparent diffusion coefficients in the evaluation of brain tumors.** *Euro J Radiol* 2005;55:393–400
25. Reiche W, Hagen T, Schuchardt V, et al. **Diffusion-weighted MR imaging improves diagnosis of CNS lymphomas: a report of four cases with common and uncommon imaging features.** *Clin Neurol Neurosurg* 2007;109:92–101
26. Toh CH, Castillo M, Wong AM, et al. **Primary cerebral lymphoma and glioblastoma multiforme: differences in diffusion characteristics evaluated with diffusion tensor imaging.** *AJNR Am J Neuroradiol* 2008;29:471–75
27. O'Neill BP, Kelly PJ, Earle JD, et al. **Computer-assisted stereotaxic biopsy for the diagnosis of primary central nervous system lymphoma.** *Neurology* 1987;37:1160–64
28. Murray K, Kun L, Cox J. **Primary malignant lymphoma of the central nervous system, result of treatment of 11 cases and review of the literature.** *J Neurosurg* 1986;65:600–07
29. O'Neill BP, Illig JJ. **Primary central nervous system lymphoma.** *Mayo Clin Proc* 1989;64:1005–20
30. McAllister LD, Doolittle ND, Guastadisegni PE, et al. **Cognitive outcomes and long-term follow-up results after enhanced chemotherapy delivery for primary central nervous system lymphoma.** *Neurosurgery* 2000;46:51–61
31. Moffat BA, Chenevert TL, Lawrence TS, et al. **Functional diffusion map: a noninvasive MRI biomarker for early stratification of clinical brain tumor response.** *Proc Natl Acad Sci U S A* 2005;102:5524–29
32. Chenevert TL, Stegman LD, Taylor JM, et al. **Diffusion magnetic resonance imaging: an early surrogate marker of therapeutic efficacy in brain tumors.** *J Natl Cancer Inst* 2000;92:2029–36
33. Mardor Y, Pfeffer R, Spiegelmann R, et al. **Early detection of response to radiation therapy in patients with brain malignancies using conventional and high b-value diffusion-weighted magnetic resonance imaging.** *J Clin Oncol* 2003;21:1094–100
34. Hamstra DA, Chenevert TL, Moffat BA, et al. **Evaluation of the functional diffusion map as an early biomarker of time-to-progression and overall survival in high-grade glioma.** *Proc Natl Acad Sci U S A* 2005;102:16759–64